J Mol Model (2012) 18:4929–4939
DOI 10.1007/s00894-012-1483-3

ORIGINAL PAPER

The structural, electronic, and optical properties of ladder-type polyheterofluorenes: a theoretical study

Chao Zheng · Ye Tao · Jin-Zhu Cao · Run-Feng Chen · Ping Zhao · Xiao-Jun Wu · Wei Huang

Received: 24 October 2011 / Accepted: 23 May 2012 / Published online: 30 June 2012

Abstract The ladder-type polyheterofluorenes were investigated theoretically by using density functional theory (DFT) to reveal their optical and electronic properties for applications in organic optoelectronic devices. The incorporation of heteroatoms (B, Si, Ge, N, P, O, and S) into the ladder-type highly fused polyfluorene backbone can influence and modify the optoelectronic properties significantly. The functionalization on the heteroatoms allows for facile derivation and incorporation of substitutes to further tune the properties. Small geometry variations between the ground, anionic/cationic, the first excited singlet and triplet states were observed due to the very rigid ladder-type coplanar backbone. Ladder-type polycarbazole was predicted to have the highest HOMO and LUMO energy levels, polyphosphafluorene oxide have the lowest HOMO energy level, polyborafluorene have the lowest LUMO energy level and bandgap, and polysulfafluorene has the highest bandgap and triplet energy. The ladder-type carbazole and borafluorene show the highest hole and electron injection abilities respectively; while sulfafluorene has the highest electron transfer rate. Most ladder-type heterofluorenes show bipolar charge transport character suggested by the reorganization energy. All of them have significantly short effective conjugation length in comparison with linear conjugated polymers. Their absorption and emission spectra were also simulated and discussed. The diversified electronic and optical properties of the ladder-type polyheterofluorenes with the different incorporated heteroatom and the substituent on it indicate their broad potential applications in organoelectronics.

Keywords Density-functional calculations · Highly fused fluorenes · Ladder-type polyheterofluorene · Optoelectronic properties

Electronic supplementary material The online version of this article (doi:10.1007/s00894-012-1483-3) contains supplementary material, which is available to authorized users.

C. Zheng · Y. Tao · J.-Z. Cao · R.-F. Chen (✉) · X.-J. Wu · W. Huang (✉)
Key Laboratory for Organic Electronics & Information Displays (KOLED), Jiangsu-Singapore Joint Research Center on Organic/Bio- Electronics and Information Displays & Institute of Advanced Materials (IAM), Nanjing University of Posts & Telecommunications (NUPT),
9 Wenyuan Road,
Nanjing 210046, Jiangsu, China
e-mail: iamrfchen@njupt.edu.cn
e-mail: iamdirector@fudan.edu.cn

P. Zhao
Key Laboratory for Advanced Materials and Institute of Fine Chemicals, East, China University of Science & Technology,
130 Meilong Road,
Shanghai 200237, China

Introduction

Ladder-type π-conjugated systems with fused backbones have aroused continuing interests in the field of organic optoelectronic materials and related applications [1–3] because of their highly effective conjugation in the very rigid coplanar structures [4]. Due to the complete ring fusion, this class of π-conjugated molecules can provide good packing, high charge mobility, and high thermal stability with great potentials for high performance optoelectronic devices [5]. For example, pentacene [6] and its derivatives have shown the hole mobility of ~3 cm^2V^{-1} s^{-1} with on-off current ratios of about 10^8 in organic field effect transistors (OFETs), whilst the heteroatom incorporated pentacene analogues such as pentathienoacene [4], bis-silicon-bridged stilbenes [7], heteraborins [8], and diindolodithienopyrroles [1] were

also prepared by incorporating heteroatoms and solublizing groups into the acenes to improve the stability and solubility of [n]acenes (n≥5). These heteroacenes have improved device performance [1] due to their low HOMO energy levels and the facile derivation on the heteroatoms to fine tune the molecular organization and solubility [9].

Ladder-type [n]phenylenes are more stable under photo-oxidation and more soluble in common solvents than [n] acenes, and are consequently more desired molecules for plastic electronics [10]. The ladder-type fluorenes and their polymers (see Scheme 1, X=C) have been found to be emissive materials for stable pure-blue light emitting devices (OLEDs) [11], to be air-stable molecules with high charge mobility for OFETs [12], to be light-harvesting and hole-conducting materials with high open-circuit voltages and ambient photovoltaic activity for solar cells (OPVs) [13], to be two-photon absorption and related up-converted emission chromophores [14], and to be a gain medium with very low threshold value for amplified spontaneous emission (ASE) in the blue spectral region [15]. The incorporation of heteroatoms can also be an important and powerful methodology of the ongoing efforts to prepare new ladder-type [n]phenylene analogues with desired structures and properties as that in [n]acenes [16, 17]. It has been shown in the research of heterofluorenes [18–22] that any atom that can act as a second linker to make the nearby two pre-bonded benzene rings into a plane for π-conjugation, will enable the formed ladder-type [n]heterophenylenes to be electronic and/or optoelectronic materials. With this molecular design strategy, symmetric and nonsymmetric diindolocarbazoles (ladder-type carbazole) [23–25] has been synthesized and their good packing, high charge mobility, and high thermal stability has been observed due to their very rigid ladder-type backbone. Bis-silicon-bridged *p*-terphenyls (ladder-type silafluorene) have been prepared [26, 27] via different methods and were found to be efficient blue-light emitting materials. Dibenzothienobisbenzothiophenes (ladder-type sulfafluorenes) [28, 29] were reported to have the mobility up to 0.15 cm^2V^{-1} s^{-1} and on-off current ratios $>10^6$ in OFET devices. Besides these ladder-type heterofluorenes, hybrid ones [30] such as bisindenocarbazole, dibenzothienocarbazole, and diindolobenzobisbenzothiophene were also prepared and found that they have much lower HOMO energy levels and larger bandgaps compared with those of pentacene, in spite of their much more extended π system. However, despite the ladder-type fluorenes, other ladder-type heterofluorenes such as borafluorene, germafluorene, oxygafluorene and phosphafluorene were scarcely reported, mainly due to the difficulty in the establishment of efficient and practical synthetic protocols [31] for these fused structures. On account of the difficulties in synthesis of ladder-type heterofluorenes, quantum chemical calculations can provide good insight into the electronic and optical properties of known molecules and the prediction of those of yet unknown, which help to design a number of new derivatives to obtain the desired optical properties. To our knowledge, there are very few papers published in the theoretical investigations of ladder-type oligo- and poly- heterofluorenes so far.

In this paper, we provide a systematic DFT simulation on the structural, electronic, and optical properties of ladder-type [n]heterofluorenes (n is the number of phenyls, n=3, 4, 5, 6, and 7, L[n]HFs) bridged by heteroatoms of B, Si, Ge, N, P, S, and O as shown in Scheme 1. The properties of ladder-type polyheterofluorenes (n→∞, L[∞]HFs) were obtained by exponential extrapolating the corresponding parameters of the corresponding [n]heterofluorenes. The influence of ladder-type fused molecular backbone, the heteroatoms, and the substitutions on the heteroatoms were discussed and evaluated for the optoelectronic applications. This investigation suggests that L[n]HFs are very interesting optoelectronic materials with diversified frontier orbital energies, charge injection and transport, and absorption and emission spectra, which all can be effectively tuned by the heteroatom and its substituents.

Computational methods

The density functional theory (DFT) computations were carried out with Gaussian03 program package with different parameters for structure optimizations and vibration analyses. The ground state molecules were optimized by B3LYP (Becke three-parameter hybrid functional combined with Lee–Yang–Parr correlation functional) formalism at the standard split valence plus polarization function 6-31 G(d) basis set. The lowest triplet (T_1), cationic (^+D), and anionic (^-D) states of the molecules were optimized by the unrestricted formalism (UB3LYP)/ 6-31 G(d). The first excited singlet state (S_1) geometries were optimized by the *ab initio* configuration interaction singles method (CIS). The fully

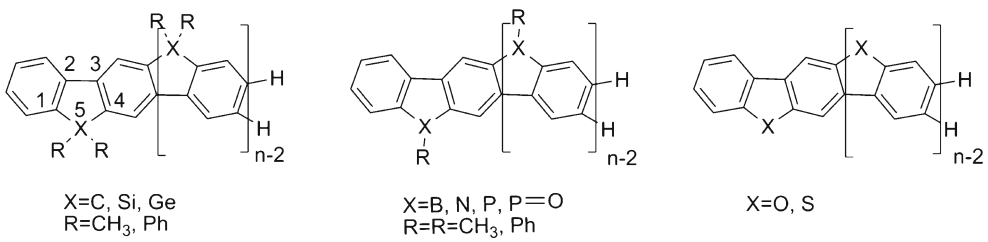

Scheme 1 The molecular structures of the ladder-type [n]heterofluorenes (n=3, 4, 5, 6, 7)

optimized stationary points were further characterized by harmonic vibrational frequency analysis to ensure that real local minima had been found without imaginary vibrational frequency. The charge (hole and electron) mobility of the L[n]HFs was assessed by using the Marcus theory based on the incoherent hopping model. According to Marcus theory [31], the rates of charge transfer can be characterized by hole/electron (h/e) reorganization energy ($\lambda_{h/e}$, the energy associated with relaxing the geometry of the system after charge transfer) and the lower the $\lambda_{h/e}$ the higher the charge transfer rate. The $\lambda_{h/e}$s were calculated according to the literature reports.

$$\lambda_h = [E^+(A) - E^+(A^+)] + [E(A^+) - E(A)] \quad (1)$$

$$\lambda_e = [E^-(A) - E^-(A^-)] + [E(A^-) - E(A)], \quad (2)$$

where E^+, E, and E^- represent the energies of the cation, neutral, and anion species based on the different geometries of (A^+), (A), and (A^-) which denote the optimized structures at corresponding cation, neutral, and anion states.

The electronic absorption and emission spectra in vacuum were carried out using the time-dependent density functional theory (TDDFT) method of B3LYP/6-31 G(d) on the basis of the optimized ground (S_0) and the first excited (S_1) structures. The electronic absorption and emission spectra were simulated by Gaussian functions with a half-width of 3000 cm^{-1} based on the 20 lowest singlet energies from TDDFT/B3LYP/6-31(d) calculations. From the optimized S_0, S_1, T_1, ^+D, and ^-D states of L[n]HFs, the various property parameters such as the highest occupied molecular orbital (HOMO), the lowest unoccupied molecular orbital (LUMO), energy gap (E_g), triplet energy (^3E_g), singlet excitation energy (E_{S1}), triplet excitation energy (E_{T1}), ionization potential (IP), electron affinity (EA), and reorganization energy (λ), were derived from the computed results according to literature publications [32–36]. The energy bandgap (E_g) is equal to the difference between the LUMO energy (E_{LUMO}) and HOMO energy (E_{HOMO}), i.e., $E_g=E_{LUMO}-E_{HOMO}$. The E_{S1} was excitation energy from S_0 to S_1. Both E_g and E_{S1} were used to assess the electronic bandgap of the ladder-type heterofluorenes. Also, two methods were used to predict the lowest triplet state (T_1) energy. One is E_{T1} obtained from the excitation energy from S_0 to T_1 and the other is ^3E_g obtained from the total molecular energy difference between T_1 and S_0. The IP and EA is the energy difference between the ionic state and the ground state. The property parameters of L[∞]HFs of E_{LUMO}, E_{HOMO}, E_g, and absorption wavelength were obtained by extrapolating the corresponding parameters of the equation from the calculated ones of n=3, 4, 5, 6, and 7 (in Tables S1 and S2): y=y0+A1*exp(−n/t1), where y0 is for the polymer when n→∞. Good coincidence with this equation fitting was observed with the corresponding coefficient of determination-adjusted R-squares (Adj.R^2) all above 0.99 (see Table S1). The effective conjugation length (L) of the ladder-type conjugated polymers were defined as the number of phenyl in the backbone (n) at 95 % and 99 % value of a particular parameters of the polymers (L=n, when y=95 % or 99 % of y0).

Results and discussion

The optimized geometries of the ladder-type heterofluoenes

The geometries of L[n]HFs at the ground, first singlet and triplet, and cationic and anionic states have been optimized and listed in Table 1. The singlet excited states (S_1) data of several compounds were absent due to their unconverged optimization. The heteroaromatic polyconjugated systems have the analytic form of a linear combination of ring C=C/C-C stretching, which points in the direction from a benzenoid structure (ground electronic state) to a quinoid one (excited electronic state). All the molecules are planar at all these states. From Table 1, the key geometries of the central heterole structure in L[n]HFs are very close to that in heterofluorenes [32] at the ground state (S_0). At the lowest excited singlet and triplet states (S_1 and T_1), the main structural variation also occurs at the heterole structure with elongated C1-C2 bond ($R_{1,2}$) and shortened C2-C3 bond ($R_{2,3}$). However, in comparison with the heterofluorenes, the corresponding ladder-type ones have significantly reduced structural rearrangement due to the highly rigid and fused molecular backbone of the ladder structure, suggesting that they are hardly affected by the lattice relations taking place. The structural variation from S_0 to T_1 is larger than that to S_1 since T_1 has lower energy level with more relaxed geometry. At the charged states, two types of geometry relaxation can be observed. The first one is concentrated on the heteroatom and its substituents with greatly varied (>0.01 Å) bond lengths of C1-X ($R_{1,5}$) due to the high electron or hole affinity of the heteroatom group such as Si, N, PO, and S. The second one focuses on the heterole backbone with elongated C1-C2 bond ($R_{1,2}$) and shortened C2-C3 bond ($R_{2,3}$) like that at the excited states. Phenyl and methyl substituents on the heteroatoms can affect $R_{1,5}$ in borafluorene and fluorene to some extent, but have almost neglectable influence on the geometries of L[n]HFs as that been observed and explained in heterofluorenes [32]. When the number of benzene rings increases from 3 to 7, L[n]HFs have very small geometry changes with the bond length ratio variation below 4‰. The rigid planar L[n]HFs with minor structural adjustments upon excitation and charge injection will offer this kind of material with particular properties, which will be discussed in the next sections.

Table 1 The optimized geometric parameters of the ladder-type [3]diheterofluorenes (L[3]HFs, shown in Scheme 1) at ground (S_0), anionic ($^-$D), cationic ($^+$D), lowest singlet (S_1) and triplet (T_1) excited states (bond lengths in Å, and angles in degree)

L[3]HF	State	$R_{1,5}$	$R_{1,2}$	$R_{2,3}$	$A_{1,5,4}$	L[3]HF	State	$R_{1,5}$	$R_{1,2}$	$R_{2,3}$	$A_{1,5,4}$
MeB	S_0	1.567	1.422	1.488	103.6	PhB	S_0	1.571	1.423	1.486	103.8
	S_1	1.563	1.425	1.438	102.6		S_1	1.563	1.425	1.438	102.8
	T_1	1.564	1.441	1.439	103.0		T_1	1.565	1.441	1.438	103.2
	$^+$D	1.568	1.436	1.453	102.5		$^+$D	1.574	1.436	1.450	102.5
	$^-$D	1.572	1.432	1.474	103.9		$^-$D	1.573	1.431	1.474	104.1
MeC	S_0	1.528	1.410	1.467	101.3	PhC	S_0	1.541	1.408	1.465	100.7
	S_1	1.526	1.422	1.413	100.9		S_1				
	T_1	1.523	1.437	1.407	101.3		T_1	1.542	1.436	1.406	100.7
	$^+$D	1.525	1.424	1.434	100.8		$^+$D	1.535	1.422	1.436	100.4
	$^-$D	1.531	1.428	1.434	101.8		$^-$D	1.545	1.426	1.433	101.1
MeSi	S_0	1.885	1.420	1.487	91.4	PhSi	S_0	1.885	1.419	1.487	91.2
	S_1	1.879	1.432	1.431	90.2		S_1				
	T_1	1.883	1.448	1.423	90.8		T_1	1.883	1.447	1.424	90.7
	$^+$D	1.893	1.434	1.452	89.7		$^+$D	1.896	1.433	1.452	89.4
	$^-$D	1.875	1.442	1.451	92.2		$^-$D	1.874	1.438	1.456	92.1
MeGe	S_0	1.940	1.417	1.487	89.9	PhGe	S_0	1.939	1.416	1.487	89.9
	S_1	1.935	1.431	1.430	88.9		S_1				
	T_1	1.938	1.446	1.421	89.6		T_1	1.937	1.445	1.422	89.6
	$^+$D	1.947	1.431	1.452	88.3		$^+$D	1.949	1.430	1.452	88.1
	$^-$D	1.932	1.439	1.449	90.9		$^-$D	1.929	1.436	1.452	90.9
MeN	S_0	1.388	1.422	1.447	108.8	PhN	S_0	1.398	1.419	1.448	108.5
	S_1	1.375	1.431	1.400	109.0		S_1	1.380	1.429	1.400	108.9
	T_1	1.398	1.430	1.429	109.7		T_1	1.398	1.434	1.423	109.1
	$^+$D	1.404	1.415	1.455	109.5		$^+$D	1.409	1.415	1.455	109.2
	$^-$D	1.393	1.436	1.425	109.4		$^-$D	1.412	1.431	1.424	108.7
MeP	S_0	1.840	1.415	1.470	89.2	PhP	S_0	1.841	1.414	1.471	89.2
	S_1	1.833	1.427	1.418	88.6		S_1				
	T_1	1.844	1.443	1.410	88.8		T_1	1.844	1.443	1.410	88.7
	$^+$D	1.839	1.431	1.437	88.4		$^+$D	1.838	1.430	1.438	88.3
	$^-$D	1.840	1.435	1.436	89.6		$^-$D	1.845	1.433	1.437	89.6
MePO	S_0	1.827	1.412	1.481	91.2	PhPO	S_0	1.827	1.411	1.481	91.1
	S_1	1.808	1.423	1.426	90.6		S_1				
	T_1	1.824	1.439	1.419	90.8		T_1	1.822	1.438	1.421	90.6
	$^+$D	1.834	1.427	1.447	90.1		$^+$D	1.833	1.427	1.449	90.0
	$^-$D	1.818	1.430	1.448	91.7		$^-$D	1.816	1.428	1.451	91.6
O	S_0	1.375	1.408	1.451	106.1	S	S_0	1.769	1.413	1.455	91.0
	S_1	1.356	1.416	1.404	107.2		S_1	1.760	1.424	1.406	91.1
	T_1	1.375	1.434	1.398	106.5		T_1	1.763	1.442	1.402	91.2
	$^+$D	1.372	1.424	1.418	106.2		$^+$D	1.757	1.417	1.458	92.1
	$^-$D	1.379	1.423	1.426	106.3		$^-$D	1.778	1.429	1.426	91.6

* The names of ladder-type heterofluorenes in this table are abbreviated. Me and Ph represent the methyl and phenyl substituents respectively on the heteroatom of heterofluorenes: B-borafluorene, C-fluorene, Si-silafluorene, Ge- germafluorene, N- carbazole, P- phosphafluorene, PO-phosphafluorene oxide, O-oxygafluorene and S- sulfafluorene

Frontier molecular orbitals

From Table 2, ladder-type [3]carbazoles (MeN and PhN) have the highest HOMO and LUMO energy levels, which coincides with the fact that carbazole is the core-building unit for hole-transporting materials [37, 38]. By replacing nitrogen with other heteroatoms, the resulting ladder-type [3]heterofluorenes show both decreased HOMO and LUMO

Table 2 HOMO and LUMO energies (E_{HOMO} and E_{LUMO}), energy bandgap (E_g), singlet excitation energy (E_{S1}), triplet state energy (^3E_g), triplet excitation energy (E_{T1}), ionization potentials (IP),electron affinities (EA),reorganization energy of hole transfer (λ_h),reorganization energy of electron transfer (λ_e) of the ladder-type [3]heterofluorenes (L[3]HF) (in eV)

L[3]HF	E_{HOMO}	E_{LUMO}	E_g	E_{S1}	^3E_g	E_{T1}	$^3E_g/E_g$	IP	EA	λ_h	λ_e
MeB	−5.39	−2.50	2.90	2.19	1.49	1.62	0.51	6.68	−1.26	0.23	0.22
MeC	−5.32	−1.09	4.23	3.91	2.59	2.66	0.61	6.59	0.13	0.23	0.26
MeSi	−5.39	−1.27	4.12	3.65	2.45	2.55	0.59	6.59	−0.12	0.29	0.31
MeGe	−5.40	−1.21	4.19	3.77	2.51	2.60	0.60	6.59	−0.07	0.30	0.33
MeN	−4.79	−0.97	3.82	3.30	2.63	2.65	0.69	6.10	0.30	0.21	0.22
MeP	−5.61	−1.38	4.24	3.81	2.58	2.66	0.61	6.85	−0.19	0.26	0.30
MePO	−6.12	−2.05	4.07	3.55	2.42	2.52	0.59	7.34	−1.02	0.29	0.48
O	−5.72	−1.40	4.32	3.95	2.76	2.80	0.64	7.07	−0.07	0.24	0.22
S	−5.57	−1.43	4.14	3.58	2.76	2.78	0.67	6.96	−0.17	0.12	0.25
PhB	−5.38	−2.65	2.73	2.04	1.44	1.55	0.53	6.53	−1.54	0.28	0.15
PhC	−5.40	−1.21	4.19	3.81	2.58	2.64	0.62	6.49	−0.14	0.23	0.26
PhSi	−5.44	−1.40	4.05	3.54	2.42	2.52	0.60	6.50	−0.42	0.32	0.31
PhGe	−5.47	−1.32	4.15	3.69	2.49	2.58	0.60	6.52	−0.34	0.35	0.35
PhN	−4.84	−1.01	3.83	3.30	2.65	2.68	0.69	6.01	0.12	0.15	0.28
PhP	−5.58	−1.34	4.24	3.79	2.59	2.66	0.61	6.71	−0.28	0.25	1.20
PhPO	−6.04	−2.03	4.02	3.47	2.38	2.49	0.59	7.17	−0.96	0.27	0.37

energy levels in the order that N>B~C~Si~Ge>S>P>O> PO and N>C>Ge>Si~P~O~S>PO respectively, which are very coincident with the changing order that found in heterofluorenes and can be explained by the HOMO-LUMO interaction theory [32]. The electronic bandgap can be investigated by the lowest singlet excitation energy (E_{S1}) and the energy bandgap (E_g), and the lowest triplet state (T_1) energy can be assessed by the lowest triplet excitation energy (E_{T1}) and the triplet energy (^3E_g). In comparison with E_g and ^3E_g, E_{S1} is slightly lower than E_g, while E_{T1} is a little higher than ^3E_g, but both pairs correlate qualitatively well with each other. The influences of the methyl and phenyl substituents of the heteroatoms on the optical and electronic properties of the ladder-type [n]heterofluorenes are very limited, but O has significant effects, resulting in much reduced LUMO and HOMO energy levels of [3] phosphafluorene oxide.

After extrapolating the energy levels of HOMOs and LUMOs of L[n]HFs (see Table S1 in the supporting information, n=3, 4, 5, 6, 7) to the polymers (n=∞), 2-14 % and 15-34 % decrements of the E_{HOMO} and E_{LUMO} were observed respectively. In all the studied ladder-type polymers (see Table 3), polycarbazole has the highest E_{HOMO} and E_{LUMO}, polyphosphafluorene oxide has the lowest E_{HOMO}, polyborafluorene has the lowest E_{LUMO} and E_g (or E_{S1}), and polysulfafluorene has the highest ^3E_g (or E_{T1}), suggesting the diversified optoelectronic properties and potential applications of the corresponding ladder-type polyheterofluorenes. From the fitting equation of L[n]HFs in Table 3, the effective conjugation length (L=n, the number of phenyl in

Table 3 HOMO and LUMO energies (E_{HOMO} and E_{LUMO}), energy bandgap (E_g), singlet excitation energy (E_{S1}), triplet state energy (^3E_g), triplet excitation energy (E_{T1}), absorption peak (Abs.), and their corresponding conjugation length (L=n at the 95 %/99 % value of the polymer) of the ladder-type polyheterofluorenes (L[∞]HFs) calculated by extrapolating the equation: y=y0+A1*exp(−n/t1) (n→∞) (in eV)

L[∞]HF	E_{HOMO}	L_H	E_{LUMO}	L_L	E_g	E_{S1}	L_E	^3E_g	E_{T1}	L_{E3}	Abs**.	L_A
MeB	−4.89	4.5/7.7	−2.96	4.8/7.2	1.41	1.93	7.0/9.8	1.00	1.03	6.0/8.1	917*	8.1/12
MeC	−4.70	5.3/9.2	−1.55	6.4/9.5	2.75	3.16	7.1/11	2.13	2.19	5.1/7.6	467	9.6/15
MeSi	−4.83	4.8/8.6	−1.70	6.7/10	2.74	3.13	7.2/11	2.07	2.13	4.6/6.9	464	8.3/13
MeGe	−4.86	4.6/7.9	−1.65	6.8/10	2.79	3.21	6.8/10	2.12	2.18	4.6/7.0	456	8.6/14
MeN	−4.19	4.8/7.5	−1.41	6.6/9.7	2.42	2.78	6.6/9.5	1.99	2.07	5.8/8.4	522*	7.2/11
MeP	−5.20	3.8/6.7	−1.97	7.4/11	2.81	3.25	6.8/10	2.18	2.25	4.7/7.1	452	9.1/15
MePO	−5.97	1.5/4.3	−2.87	7.2/11	2.71	3.10	7.1/11	2.05	2.11	4.5/6.6	465	7.6/12
O	−5.35	3.5/6.3	−2.15	8.1/12	2.71	3.23	7.2/11	2.24	2.31	5.3/8.1	485	13/21
S	−5.44	2.2/3.9	−2.17	7.5/11	2.90	3.29	6.2/9.4	2.30	2.63	4.9/7.5	430*	6.0/9.5

*with low oscillator strength (f)

**absorption peak with the highest oscillator strength (f)

the backbone) of E_{LUMO}, E_{LUMO}, and energy bandgap (E_g) can be calculated respectively at 95 % and 99 % value of the above parameters of the polymers. E_{HOMO} has shorter effective conjugation length than E_{LUMO}, which is more apparent in the cases of MeP, MePO, O, and S, suggesting that the electron is more delocalized than hole on the ladder-type conjugated polymer chain and P, O, and S incorporation leads to a much more localized hole. When the number of phenyl in the polymer main-chain is higher than 10, L[10]HFs have similar electronic structures of the corresponding polymers due to the shorter Ls than that in common linear conjugated polymers such as polyfluorenes (n=24) [39].

The isosurfaces of wave functions of the frontier orbitals of L[3]HFs at various states of S_0, S_1, $^-$D, and $^+$D were illustrated in Figs. 1 and S1. At the ground state (S_0), three types of electronic density distributions can be observed according to their shapes. The first type has three/three pairs of positive and negative wave functions laid vertically on the backbone in HOMO and four/four horizontal wave functions in LUMO, as found in MeB, MeSi, and MePO. The second one has three/three vertical wave functions in HOMO and four/six horizontal wave functions in LUMO, as in MeC, MeGe, MeP, and O. The third one has three/three tilted wave functions in HOMO and four/six horizontal wave functions in LUMO, as in MeN and S. These different wave function patterns are due to the different interactions between the ladder-type benzene backbone and the heteroatom, which have been explained by the HOMO-LUMO interaction theory in our previous publication [32]. At the excited singlet state (S_1), most L[3]HFs have the same electronic density configuration both in HOMO and LUMO, except for MeN, PhN, and S which have different electron distribution patterns of HOMO. This electron re-assignment in HOMO at the excited state indicates the different reactivities and stabilities of these L[3]HFs when they are excited via photo absorption or other methods. At the anionic

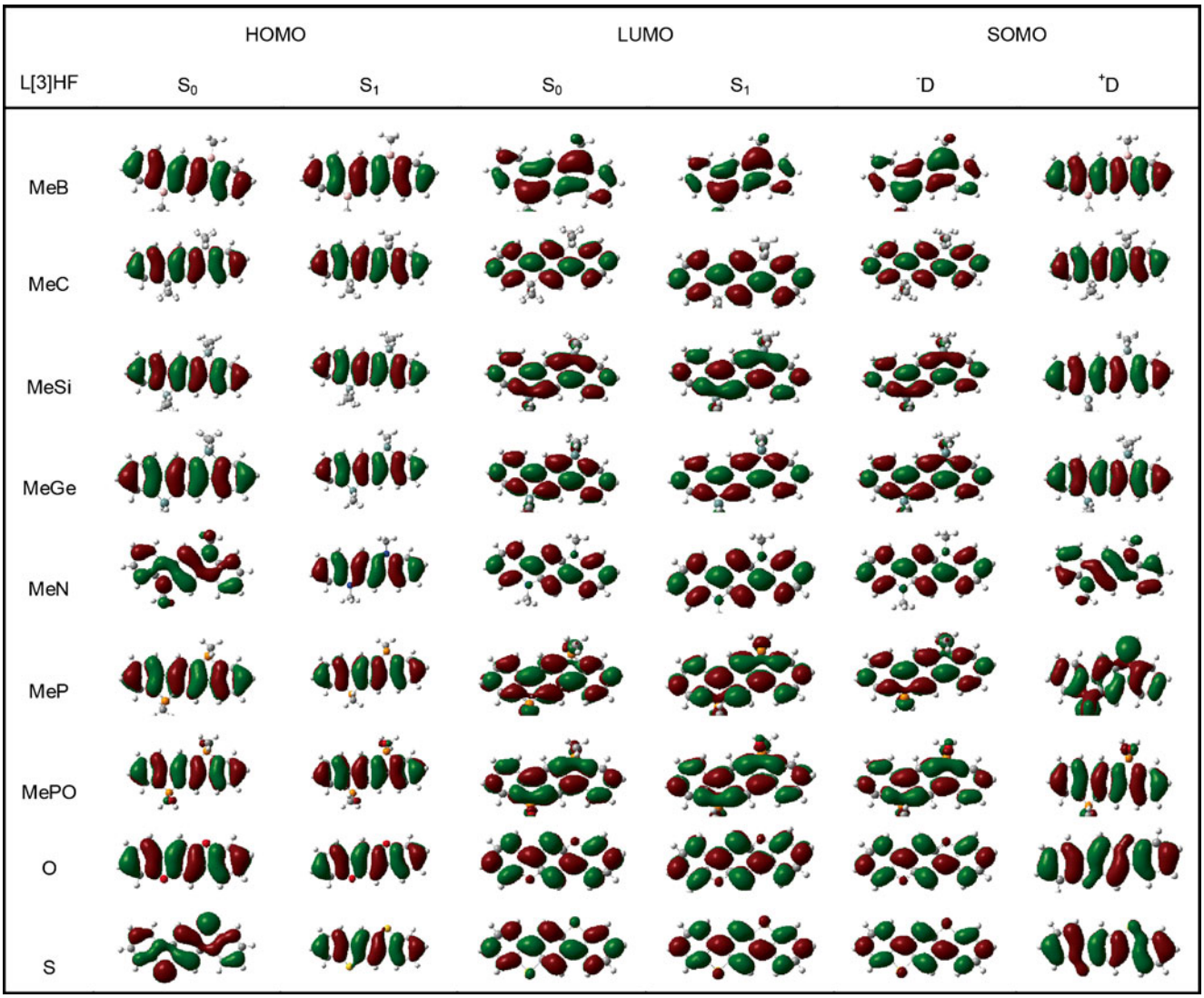

Fig. 1 The electronic densities of HOMO, LUMO and SOMO of the ladder-type [3]heteroflorenes (L[3]HFs) at different states of S_0, S_1, $^-$D, and $^+$D

state ($^{-}$D), the contour plots of SOMO of L[3]HFs are very alike to that of their LUMO at S_0 and S_1, since they are at the same molecular orbital. At the cationic state ($^{+}$D), most of their SOMOs are almost the same as their HOMOs at S_0 and S_1 except for MeN, PhN, PhP, MeP, and S, due to the stronger electron donating abilities of the heteroatoms which localize the hole and disturb the electronic density distributions.

Ionization potential, electron affinity, and reorganization energy

The charge injection and transport, and their balance are the most important properties of optoelectronic compounds. According to Marcus theory, the rates of charge transfer can be determined by hole/electron (h/e) reorganization energy ($\lambda_{h/e}$, the energy associated with relaxing the geometry of the system after charge transfer) and electronic coupling matrix element ($V_{h/e}$, depending on the overlap of the wave functions of the two states involved in the charge transfer process). Experimentally, $V_{h/e}$ shows a rather narrow range of values, and an even more limited range of $V_{h/e}$ is expected due to the direct contacts in the amorphous polymer solid films [39]. As a result, the hole/electron mobility of the silafluorene trimers in this study is considered to be dominated by $\lambda_{h/e}$ without regard for $V_{h/e}$. Investigations on the ionization potentials (IP), electronic affinities (EA), and reorganization energies ($\lambda_{h/e}$) can help us evaluate the energy barrier for charge injection and transport, as well as better understand the hole and electron transport process.

From Table 2, MeN and PhN have the lowest IPs, suggesting their highest hole injection ability, while MeB and PhB have the lowest EAs, indicating their highest electron injection ability. These findings are in accordance with the experimental observations in carbazoles and borafluorenes and also with our previous investigations [32]. The highest hole transfer rate was found in S with the lowest λ_h, while the highest electron transfer rate was found in MeB/PhB, MeN, and O with the lowest λ_e. Except for MePO, S, PhN, PhP, and PhPO (hole transport-dominate with lower λ_h than λ_e) and PhB (electron transport-dominate with lower λ_e than λ_h), the other ladder-type [3]heteroflorenes all have the adjacent λ_h and λ_e, indicating that they are bipolar charge transport materials. The phenyl substitution generally leads

Table 4 Electronic transition data obtained by TDDFT methods (TD-B3LYP/6-31 G* //B3LYP/6-31 G*) for the ladder-type [3]heterofluorenes (L[3]HFs)

L[3]HF	Electronic transitions	Wavelength /nm	f	Main configurations	Exp.
MeB	$S_1 \leftarrow S_0$	567	0.00	HOMO→LUMO (45 %)	
	$S_8 \leftarrow S_0$	288	1.25	HOMO→LUMO+2 (24 %)	
MeC	$S_1 \leftarrow S_0$	317	0.82	HOMO→LUMO (42 %)	338 [41]
MeSi	$S_1 \leftarrow S_0$	339	0.32	HOMO→LUMO (40 %)	362 [27]
	$S_7 \leftarrow S_0$	255	0.38	HOMO-1→LUMO (36 %)	
MeGe	$S_1 \leftarrow S_0$	329	0.44	HOMO→LUMO (40 %)	
MeN	$S_1 \leftarrow S_0$	376	0.04	HOMO→LUMO (44 %)	388 [42]
	$S_5 \leftarrow S_0$	262	1.17	HOMO→LUMO+2 (39 %)	
MeP	$S_1 \leftarrow S_0$	325	0.39	HOMO→LUMO (33 %)	
MePO	$S_1 \leftarrow S_0$	348	0.23	HOMO→LUMO (41 %)	
	$S_4 \leftarrow S_0$	286	0.28	HOMO-1→LUMO (18 %)	
PhB	$S_1 \leftarrow S_0$	607	0.00	HOMO→LUMO (46 %)	
(HOMO→LUMO+2 (19 %))	$S_{10} \leftarrow S_0$	302	0.66	HOMO-8→LUMO (17 %)	
PhC	$S_1 \leftarrow S_0$	325	0.60	HOMO→LUMO (42 %)	347 [43]
PhSi	$S_1 \leftarrow S_0$	350	0.22	HOMO→LUMO (42 %)	
	$S_9 \leftarrow S_0$	265	0.37	HOMO-1→LUMO(23 %)	
PhGe	$S_1 \leftarrow S_0$	336	0.33	HOMO→LUMO(40 %)	
PhN	$S_1 \leftarrow S_0$	375	0.04	HOMO→LUMO(45 %)	422 [42]
	$S_{13} \leftarrow S_0$	263	0.91	HOMO→LUMO+6(38 %)	
PhP	$S_1 \leftarrow S_0$	327	0.35	HOMO→LUMO(34 %)	
PhPO	$S_1 \leftarrow S_0$	357	0.17	HOMO→LUMO(42 %)	
	$S_8 \leftarrow S_0$	279	0.54	HOMO-1→LUMO(24 %)	
O	$S_1 \leftarrow S_0$	314	0.05	HOMO-1→LUMO(42 %)	354 [42]
	$S_2 \leftarrow S_0$	308	0.82	HOMO→LUMO(41 %)	
S	$S_1 \leftarrow S_0$	346	0.04	HOMO→LUMO(44 %)	369 [44]
	$S_7 \leftarrow S_0$	253	0.82	HOMO→LUMO+2(35 %)	

to lower IP and EA but lower charge mobility with higher $\lambda_{h/e}$ (except for PhB and PhN), corresponding to better hole and electron injection but worse transport properties in comparison with the methyl substituent.

Absorption spectra

In order to understand the optical properties of L[n]HFs, TDDFT calculations on the absorption and emission spectra in vacuum were performed. The calculated absorption wavelengths, main transition configurations, and oscillator strengths for the most relevant excited states of the ladder-type [3]heteroflorenes were listed in Table 4. From Table 4 and the MOs in Fig. 2, all of the electronic transitions of L[3]HFs are of the $\pi \rightarrow \pi^*$ type for the absorption spectra, but the electron transitions are not all from the initial state of HOMO or HOMO-1, to the final state of LUMO or LUMO+1. For MeC, PhC, MeGe, PhGe, MeP, and PhP, the $S_1 \leftarrow S_0$ transitions are predominantly π–π^* type involving delocalized HOMOs and LUMOs and have highest intensity as suggested by their largest oscillator strength (f) values. For MeB and PhB, the lowest $S_1 \leftarrow S_0$ transition involving HOMOs and LUMOs are almost forbidden due to their very small f values. Instead, they have the calculated maximum absorption from HOMO to LUMO+2 ($S_8 \leftarrow S_0$) or from HOMO-8 to LUMO ($S_{10} \leftarrow S_0$). For MeSi, PhSi, MeN, PhN, MePO, PhPO, O, and S, the lowest $S_1 \leftarrow S_0$ transition is not forbidden but relatively weaker than the higher excited state transition. For example, MeN has the strongest transition of $S_5 \leftarrow S_0$ from HOMO to LUMO+2, PhPO has that of $S_8 \leftarrow S_0$ from HOMO-1 to LUMO, and S has that of $S_7 \leftarrow S_0$ from HOMO to LUMO+2. The various electronic structures of L[3]HFs clearly demonstrate the great influence of heteroatoms on their optical properties. These calculated results are coincident well with the experimental reports shown in Table 4 with about 20 nm underestimation of UV–vis absorption peak except for PhN and O.

Figure 2 illustrates the absorption spectra of the L[n]HFs simulated by Gaussian functions with a half-width of 3000 cm^{-1} based on the 20 lowest singlet energies from TDDFT/B3LYP/6-31(d) calculations. It is noteworthy that the absorption spectra of the compounds are featured with several vibronic peaks especially for MeSi, MeGe, PhSi, and PhGe, which is characteristic of fused-ring systems with well-defined electronic states. Compared with methyl substituent, phenyl show an obvious red-shift in the UV–vis absorption (~10 nm), which is in accordance with that found in E_g (Table 2). As in MeB and PhB, a large red shift about 70 nm can be observed in Fig. 2, due to the rearrangement of the electronic transitions, showing the obvious difference between methyl- and phenyl-substituted L[3]HFs. PhB and PhPO have the longest absorption wavelength around

Table 5 The electronic transition data calculated by TDDFT methods for the PL spectra of the ladder-type [3]heterofluorenes (L[3]HFs)

L[3]HF	Electronic transitions	Wavelength /nm	f	Main configurations
MeB	$S_1 \rightarrow S_0$	729	0.01	HOMO→LUMO (44 %)
	$S_8 \rightarrow S_0$	291	1.04	HOMO-4→LUMO (20 %)
				HOMO→LUMO+2 (14 %)
MeC	$S_1 \rightarrow S_0$	353	0.92	HOMO→LUMO (40 %)
MeSi	$S_1 \rightarrow S_0$	391	0.41	HOMO→LUMO (40 %)
	$S_7 \rightarrow S_0$	264	0.41	HOMO-2→LUMO (33 %)
MeGe	$S_1 \rightarrow S_0$	376	0.55	HOMO→LUMO (40 %)
MeN	$S_1 \rightarrow S_0$	384	0.06	HOMO→LUMO (39 %)
	$S_2 \rightarrow S_0$	342	0.72	HOMO-1→LUMO (35 %)
	$S_6 \rightarrow S_0$	252	0.83	HOMO→LUMO+2 (39 %)
MeP	$S_1 \rightarrow S_0$	371	0.57	HOMO→LUMO (40 %)
MePO	$S_1 \rightarrow S_0$	405	0.31	HOMO→LUMO (40 %)
	$S_4 \rightarrow S_0$	301	0.25	HOMO-1→LUMO (17 %)
				HOMO-3→LUMO (16 %)
	$S_{11} \rightarrow S_0$	258	0.30	HOMO-8→LUMO (25 %)
O	$S_1 \rightarrow S_0$	334	0.97	HOMO→LUMO (40 %)
S	$S_1 \rightarrow S_0$	359	0.10	HOMO-1→LUMO (28 %)
	$S_2 \rightarrow S_0$	335	0.75	HOMO→LUMO (24 %)
PhB	$S_1 \rightarrow S_0$	768	0.01	HOMO→LUMO (44 %)
	$S_{10} \rightarrow S_0$	312	0.83	HOMO→LUMO+2 (21 %)
PhN	$S_1 \rightarrow S_0$	379	0.09	HOMO→LUMO (36 %)
	$S_2 \rightarrow S_0$	341	0.72	HOMO-1→LUMO (33 %)

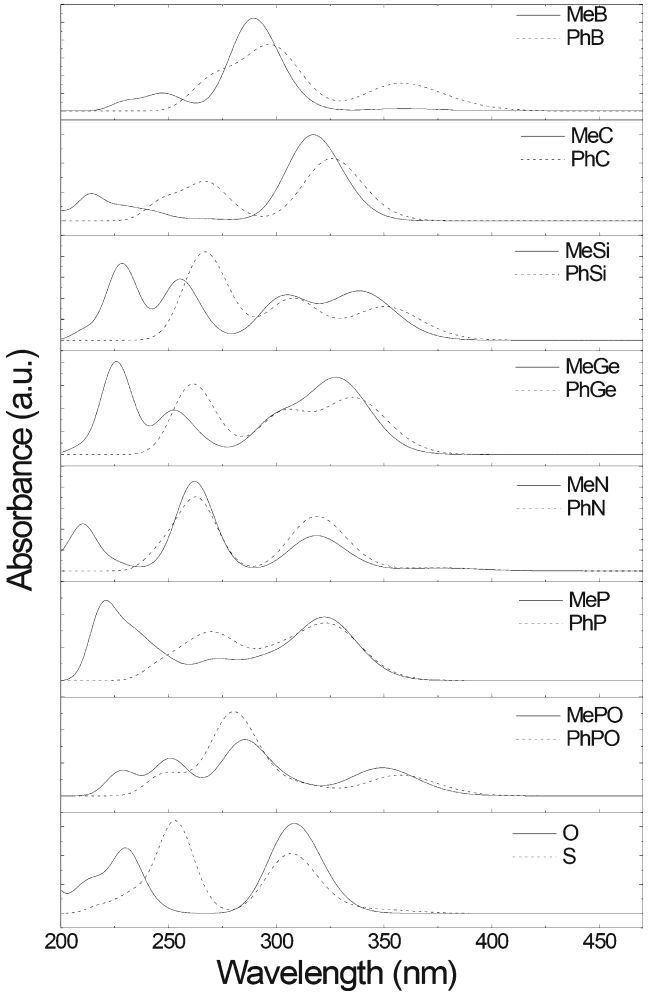

Fig. 2 The simulated absorption spectra of the ladder-type [3] heterofluorenes

360 nm. By extrapolating the wavelength of the lowest $S_0 \rightarrow S_1$ transition of the ladder-type [n]methylheterofluorenes (see Table S2 in the supporting information) to the polymers (n=∞), the longest absorption wavelength was found in MeB (917 nm), followed by MeN (522 nm), O (485 nm), MeC (467 nm), MePO (465 nm), MeSi (464 nm), MeGe (456 nm), MeP (452 nm), and S (430 nm). The effective conjugation length (at the 95 % value of the polymer (n→∞), see Table 3) of the absorption peak is lower than 10, which is in good accordance with that found in other electronic parameters. The experimental absorption band [40] of the ladder-type polymethylfluorene is around 450 nm, which is quite close to the predicted one (467 nm). However, when considering oscillator strength (f), the longest absorption band of MeB, MeN, and S may not be acceptable with f lower than 0.05. Fortunately, they all have a short conjugation length around 7 at 95 % level, which means that [7]heterofluorenes have similar (95 %) absorption peaks of the corresponding polymers. As a result, the corresponding polymers of MeB might have a maximum absorption peak around 370 nm, that of MeN is around 420 nm, and that of S is around 390 nm.

Emission spectra

The theoretical emission spectra of L[3]HFs based on CIS optimized excited-state geometries were presented in Table 5 and Fig. 3. The emission wavelengths of phenyl substituted compounds were excluded (except for PhB and PhN) because the optimizations of their excited states were not converged. From Table 5, the fluorescence ($S_0 \leftarrow S_1$) arise primarily from HOMO←LUMO π-π* de-excitations. Comparing the absorption (Fig. 2) and emission spectra (Fig. 3), mirror relation of them can be observed, indicating the small geometry variation from the ground state to the excited state, which is confirmed by the geometric data in Tables 1. The Stoke shift between S_1 and S_0 transitions various in a wide range from 160 nm (MeB and PhB), to 50 nm (MeC, MeSi, MeGe, MeP, and MePO) and 10 nm (O, S, MeN, and PhN). The small stokes shift around 10 nm is due to the rigid ladder-type planar structure, while the large one is due to the great influence of incorporated heteroatoms. Most L[3]HFs have the deep purple and blue light-emitting features (λ_{em}=330~410 nm) in vacuum, except for

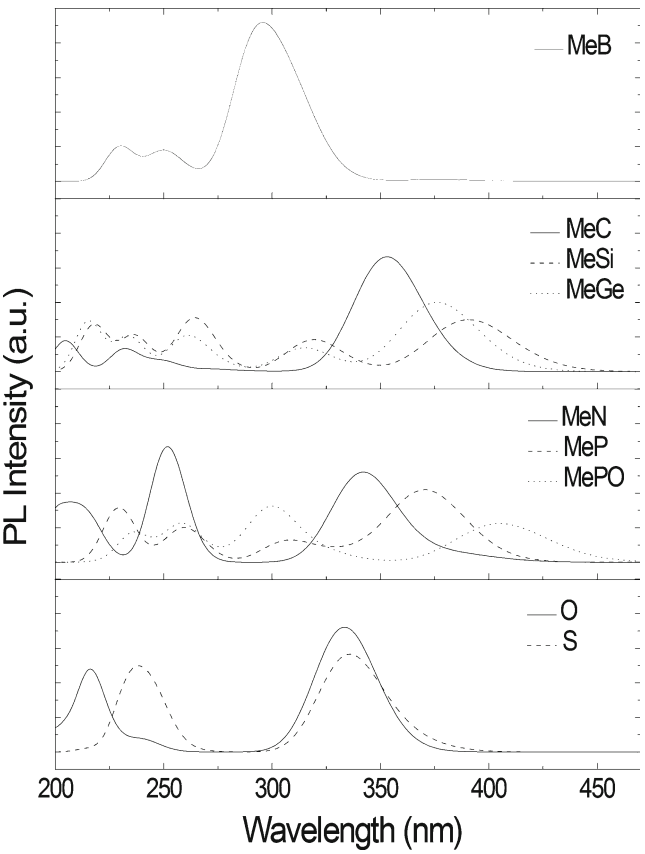

Fig. 3 The simulated photoluminescent (PL) spectra of the ladder-type [3]heterofluorenes

MeB and PhB which exhibit infrared photoluminescent (729 and 768 nm, respectively) although with very low oscillator strength (f=0.01 in Table 5), suggesting that the ladder-type polyborafluorenes may not be infrared emitters. As a result, MePO, instead of MeB and PhB, has the longest light emitting band around 410 nm, followed by MeGe, MeSi, MeN, MeC, MeN, S, and O, while MeB shows a rather blue-shifted light emitting peak around 295 nm as shown in Fig. 3. Ladder-type heterofluorenes are potential blue light-emitting materials, which is in accordance with the E_g listed in Table 3.

Conclusions

In this paper, DFT methods were adopted to investigate the structures and properties of the ladder-type polyheteroheterofluorenes (L[∞]HFs). It was found that in this ladder-type fused molecular skeleton, the heteroatom incorporation and the chemical modification of the heteroatom via methyl or phenyl substitutions and oxidation are powerful tools to tune their optoelectronic properties for the desired applications due to the effective interactions between the heteroatom and the fused benzene backbone. Ladder-type polycarbazole was predicted to have the highest HOMO (−4.19 eV) and LUMO (−1.41 eV) energy levels and hole injection ability, which enable it as potential host injection and transport materials in OLEDs. Ladder-type polyborafluorene has the lowest LUMO energy (−2.96 eV) and the highest electron injection ability to function as electron injection and transport materials. Ladder-type polysulfafluorene has the highest E_g (3.29 eV) and ^3E_g (2.63 eV) to be good host materials for green even blue-green phosphorescent emitters. The other L[∞]HFs can be high performance blue to green light emitting materials with significantly short effective conjugation length and balanced charge transport rates. In particular, L[n]HFs with highly planar molecular structure may find many applications in other optoelectronic devices such as OFETs and OPVs. These results represent a promising class of semiconducting materials of L[n]HFs, which demonstrate great potential as excellent π-conjugated systems for various optoelectronic devices.

Acknowledgments We thank the National Basic Research Program of China (2009CB930601 and 2012CB933301), National Natural Science Foundation of China (20804020, 60976019 and 20974046), The Ministry of Education of China (No. IRT1148), National Natural Science Foundation of Jiangsu Province (BK2011751), Scientific Research Foundation of Nanjing University of Posts and Telecommunications (NY210017 and NY210046), and Program for Postgraduates Research Innovations in University of Jiangsu Province (CXZZ11_0412).

References

1. Balaji G, Phua DI, Shim WL, Valiyaveettil S (2010) Org Lett 12:232–235
2. Hartley CS, Elliott EL, Moore JS (2007) J Am Chem Soc 129:4512–4513
3. Romaner L, Heimel G, Wiesenhofer H, Scandiucci de Freitas P, Scherf U, Bredas JL, Zojer E, List EJ (2004) Chem Mater 16:4667–4674
4. Malave OR, Ruiz Delgado MC, Hernandez V, Lopez Navarrete JT, Vercelli B, Zotti G, Novoa JJ, Suzuki Y, Yamaguchi S, Henssler JT, Matzger AJ (2009) Chem-Eur J 15:12346–12361
5. Huang H, Prabhakar C, Tang K, Chou P, Huang G, Yang J (2011) J Am Chem Soc 133:8028–8039
6. Kelley TW, Boardman LD, Dunbar TD, Muyres DV, Pellerite MJ, Smith TP (2003) J Phys Chem B 107:5877–5881
7. Yamaguchi S, Xu CH, Tamao K (2003) J Am Chem Soc 125:13662–13663
8. Agou T, Kobayashi J, Kawashima T (2007) Chem-Eur J 13:8051–8060
9. Niimi K, Shinamura S, Osaka I, Miyazaki E, Takimiya K (2011) J Am Chem Soc 133:8732–8739
10. Heeger AJ (2010) Chem Soc Rev 39:2354–2371
11. Jacob J, Sax S, Piok T, List EJ, Grimsdale AC, Mullen K (2004) J Am Chem Soc 126:6987–6995
12. Usta H, Facchetti A, Marks TJ (2008) J Am Chem Soc 130:8580
13. Zheng Q, Jung BJ, Sun J, Katz HE (2010) J Am Chem Soc 132:5394–5404
14. Zheng QD, Gupta SK, He GS, Tan LS, Prasad PA (2008) Adv Funct Mater 18:2770–2779
15. Laquai F, Mishra AK, Ribas MR, Petrozza A, Jacob J, Akcelrud L, Mullen K, Friend RH, Wegner G (2007) Adv Funct Mater 17:3231–3240
16. Cheedarala RK, Kim GH, Cho S, Lee J, Kim J, Song HK, Kim JY, Yang C (2011) J Mater Chem 21:843–850
17. Cheng Y, Wu J, Shih P, Chang C, Jwo P, Kao W, Hsu C (2011) Chem Mater 23:2361–2369
18. Chan KL, McKiernan MJ, Towns CR, Holmes AB (2005) J Am Chem Soc 127:7662–7663
19. Chen JW, Cao Y (2007) Macromol Rapid Comm 28:1714–1742
20. Chen RF, Zhu R, Zheng C, Liu SJ, Fan QL, Huang W (2009) Sci China Ser B 52:212–218
21. Chen RF, Zhu R, Fan QL, Huang W (2008) Org Lett 10:2913–2916
22. Chen RF, Fan QL, Zheng C, Huang W (2006) Org Lett 8:203–205
23. Bouchard J, Wakim S, Leclerc M (2004) J Org Chem 69:5705–5711
24. Tsuchimoto T, Matsubayashi H, Kaneko M, Nagase Y, Miyamura T, Shirakawa E (2008) J Am Chem Soc 130:15823–15835
25. Levesque I, Bertrand PO, Blouin N, Leclerc M, Zecchin S, Zotti G, Ratcliffe CI, Klug DD, Gao X, Gao FM, Tse JS (2007) Chem Mater 19:2128–2138
26. Li LC, Xiang JF, Xu CH (2007) Org Lett 9:4877–4879
27. Matsuda T, Kadowaki S, Goya T, Murakami M (2007) Org Lett 9:133–136
28. Sirringhaus H, Friend RH, Wang C, Ouml J, Leuninger R, Uuml KM (1999) J Mater Chem 2095–2101
29. Wang CH, Hu RR, Liang S, Chen JH, Yang Z, Pei J (2005) Tetrahedron Lett 46:8153–8157
30. Gao P, Feng XL, Yang XY, Enkelmann V, Baumgarten M, Mullen K (2008) J Org Chem 73:9207–9213
31. Marcus RA (1993) Rev Mod Phys 65:599–610
32. Chen RF, Zheng C, Fan QL, Huang W (2007) J Comput Chem 28:2091–2101
33. Yin J, Chen RF, Zhang SL, Ling Q, Huang W (2010) J Phys Chem A 114:3655–3667
34. An Z, Yin J, Shi N, Jiang H, Chen R, Shi H, Huang W (2010) J Polym Sci Pol Chem 48:3868–3879
35. Chen R, Pan J, Zhang Y, Fan Q, Huang W (2006) J Phys Chem B 110:23750–23755

36. Tao YT, Wang Q, Shang Y, Yang CL, Ao L, Qin JG, Ma DG, Shuai ZG (2009) Chem Commun 77–79
37. Boudreault PT, Eacute SB, Leclerc M (2010) Polym Chem 127–136
38. Tao Y, Wang Q, Yang C, Zhong C, Zhang K, Qin J, Ma D (2010) Adv Funct Mater 20:304–311
39. Klaerner G, Miller RD (1998) Macromolecules 31:2007–2009
40. Scherf UJ (1999) Mater Chem 9:1853–1864
41. Hertel D, Setayesh S, Nothofer HG, Scherf U, Müllen K, Bässler H (2001) Adv Mater 13:65–70
42. Kawaguchi K, Nakano K, Nozaki K (2007) J Org Chem 72:5119–5128
43. Wong K, Chi L, Huang S, Liao Y, Liu Y, Wang Y (2006) Org Lett 8:5029–5032
44. Ebata H, Miyazaki E, Yamamoto T, Takimiya K (2007) Org Lett 9:4499–4502